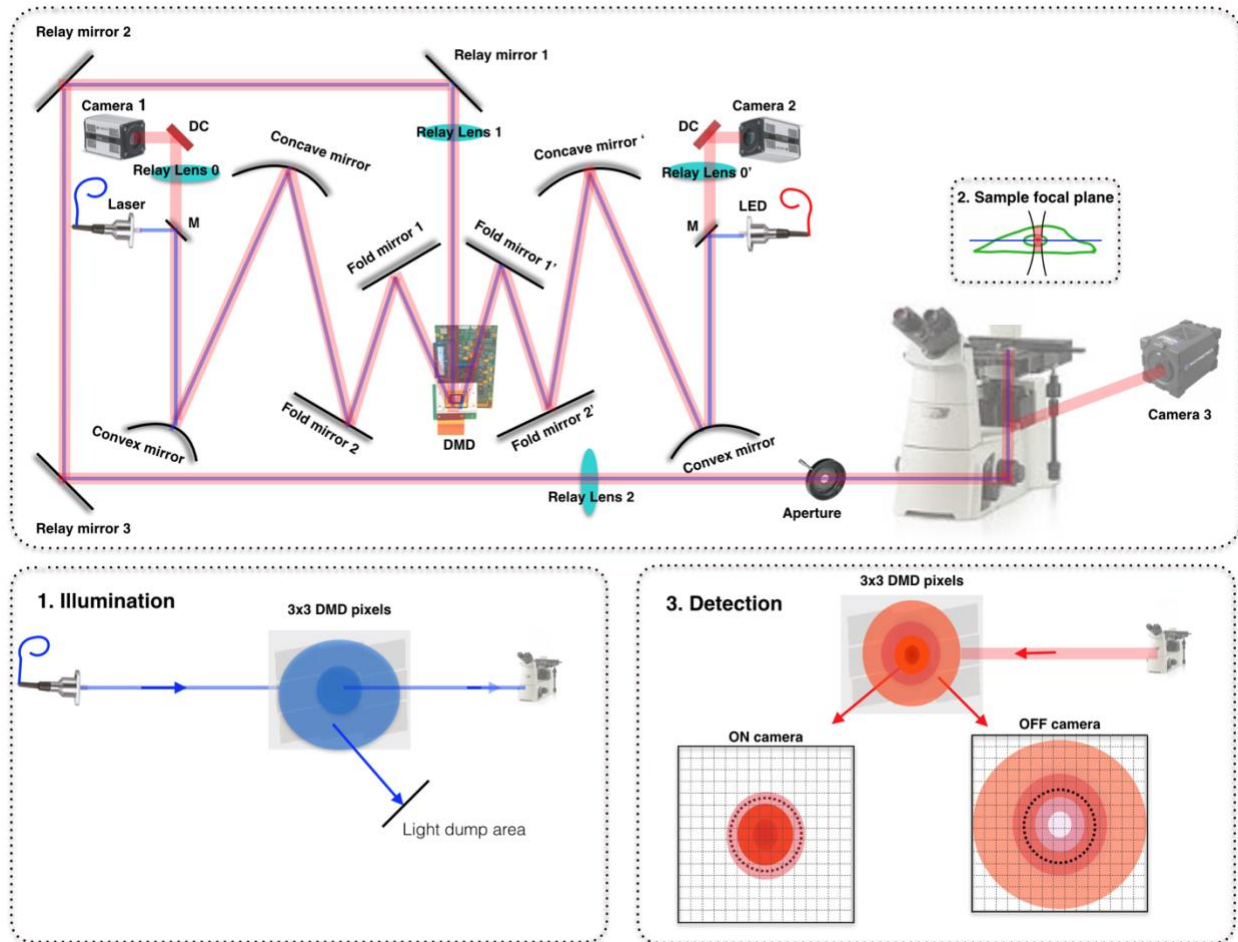


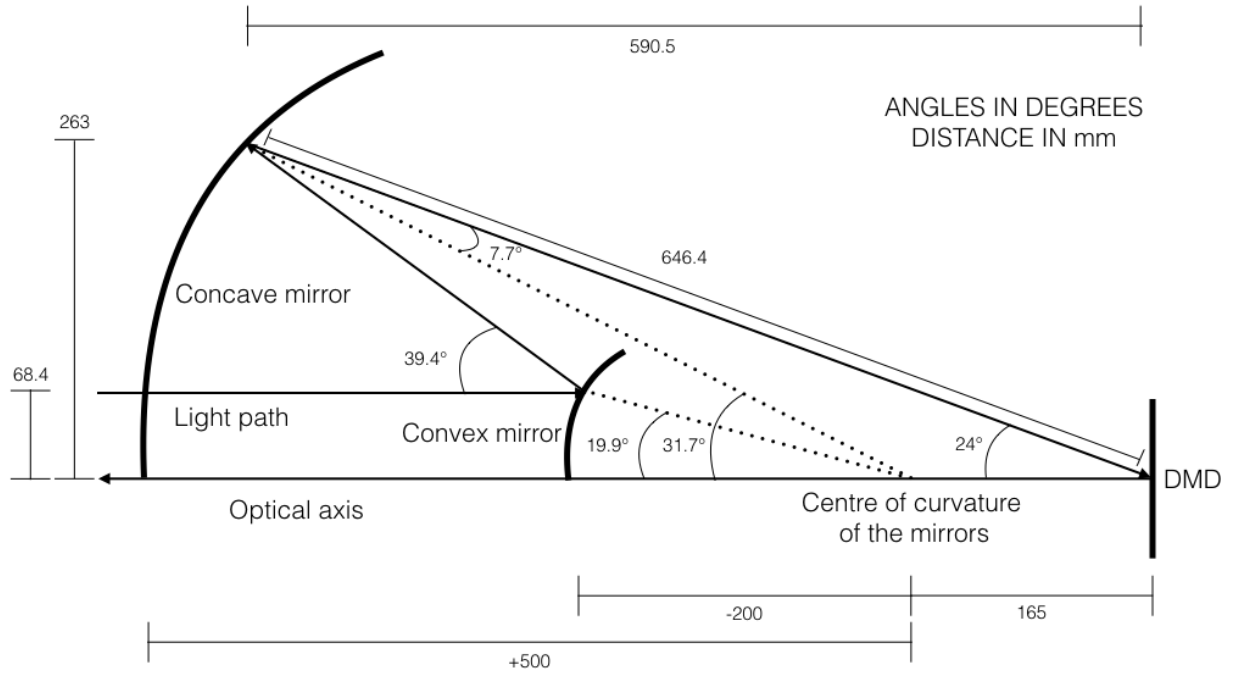
## Supplementary Figure 1. Optical set up of Super Resolution-Programmable Array Microscope (SR-PAM).



There are two illumination pathways and two detection pathways in the system. Illumination light from one of the light sources passing through an excitation filter and dichroic filter (DC) hits a convex mirror of focal length -100 mm and is reflected to a concave mirror of focal length +250 mm before projecting on to the DMD. There are two fold mirrors on each pathway between the concave mirror and the DMD to make the system compact. When light is projected on to the DMD, ON pixels (at +12 degrees) reflect light to a relay lens to form an image at the image plane of the microscope. OFF pixels (at -12 degrees) reflect light to a beam dump area inside the system (**supplementary figure 1 part 2**). When sample is illuminated (**supplementary figure 1 inset**), light from the sample passes through the system and the DMD micro-mirrors act as a physical pinhole. The major advantage of this system is that the in-focus and out-of-focus light returning from the sample can be collected separately in two separate cameras enabling the user to do advanced SR-PAM post processing techniques. The PSF collected in ON and OFF camera are shown in (**supplementary figure 1 part 3**). In-focus light coming back from the sample follows

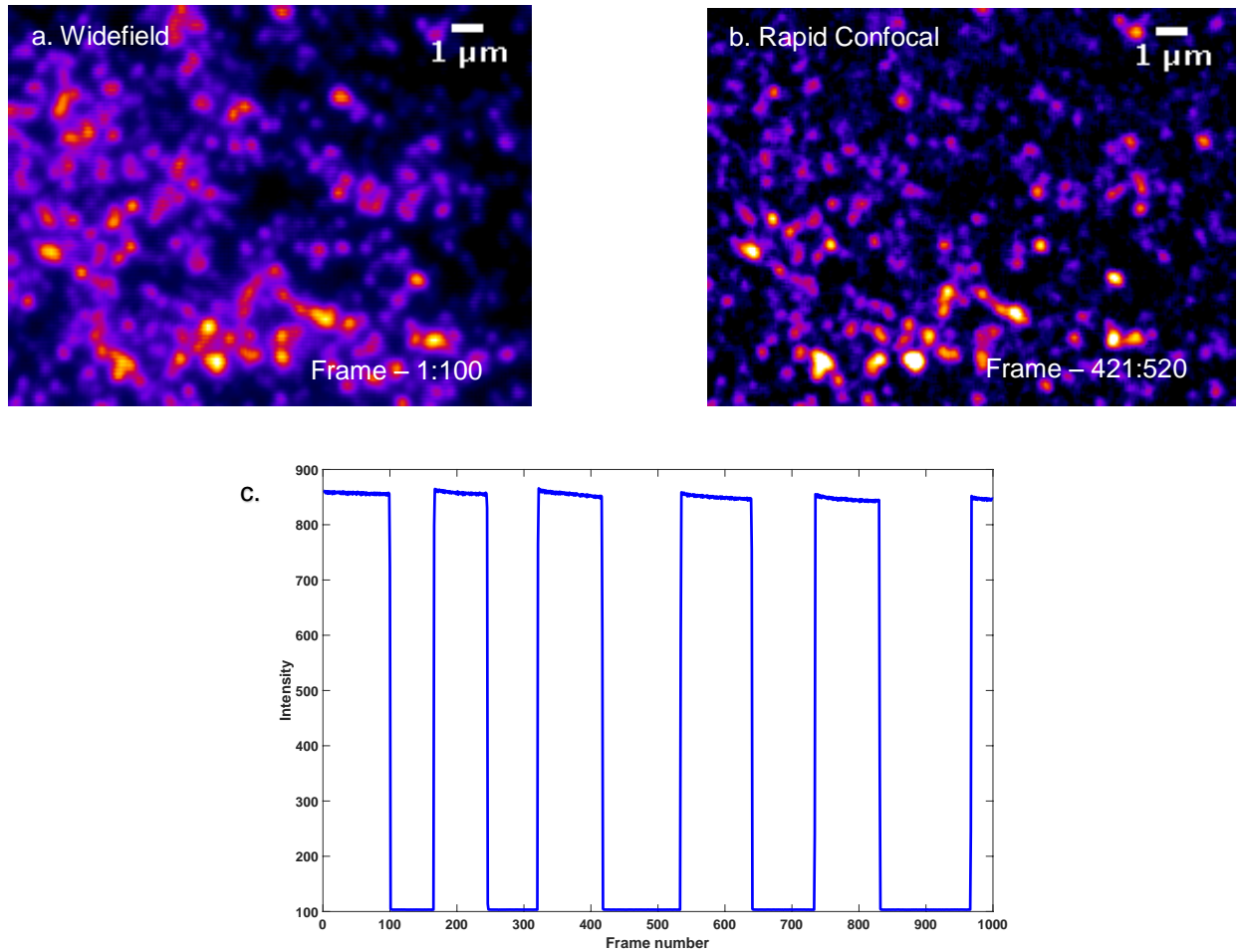
an in-focus pathway (same path as the illumination light) and gets collected in an in-focus camera (camera ON). Out-of-focus light coming back from the sample follows an out-of-focus pathway and gets collected in an out-of-focus camera (camera OFF) as described in the figure. Black dotted circle marked in the PSF collected in ON and OFF cameras (**supplementary figure 1 part 3**) is the virtual pinhole diameter, equivalent to a conventional aperture based physical pinhole confocal microscope. The system is more compact with a 3D arrangement while it is drawn as 2D for easy understanding of the optical set up. The number of optical elements is accurate but the angle, orientation and relative spacing between the optics are changed to emphasize the simplicity of the instrumentation.

## Supplementary Figure 2. Ray diagram of the light path in the optical setup



**Supplementary figure 2** illustrates the ray diagram of the optical path in the setup. Light from the illumination source hits a convex mirror of focal length -100 mm and reflects to a concave mirror at an angle  $39.4^\circ$  with respect to the incident ray to hit a concave mirror of focal length +250 mm. Centres of curvature of the two mirrors coincide and is placed at 165 mm from the DMD. Light is reflected from the concave mirror at an angle  $7.7^\circ$  with respect to the optical axis and hits the DMD. Micromirrors which are turned at an angle  $12^\circ$  with respect to the optical axis towards the light path from the concave mirror reflect the light from concave mirror hitting the micromirrors at  $24^\circ$  with respect to the optical axis along the optical axis which is relayed on to the side port of the microscope.

### Supplementary Figure 3. Switching between a point based and widefield based illumination imaging technique.



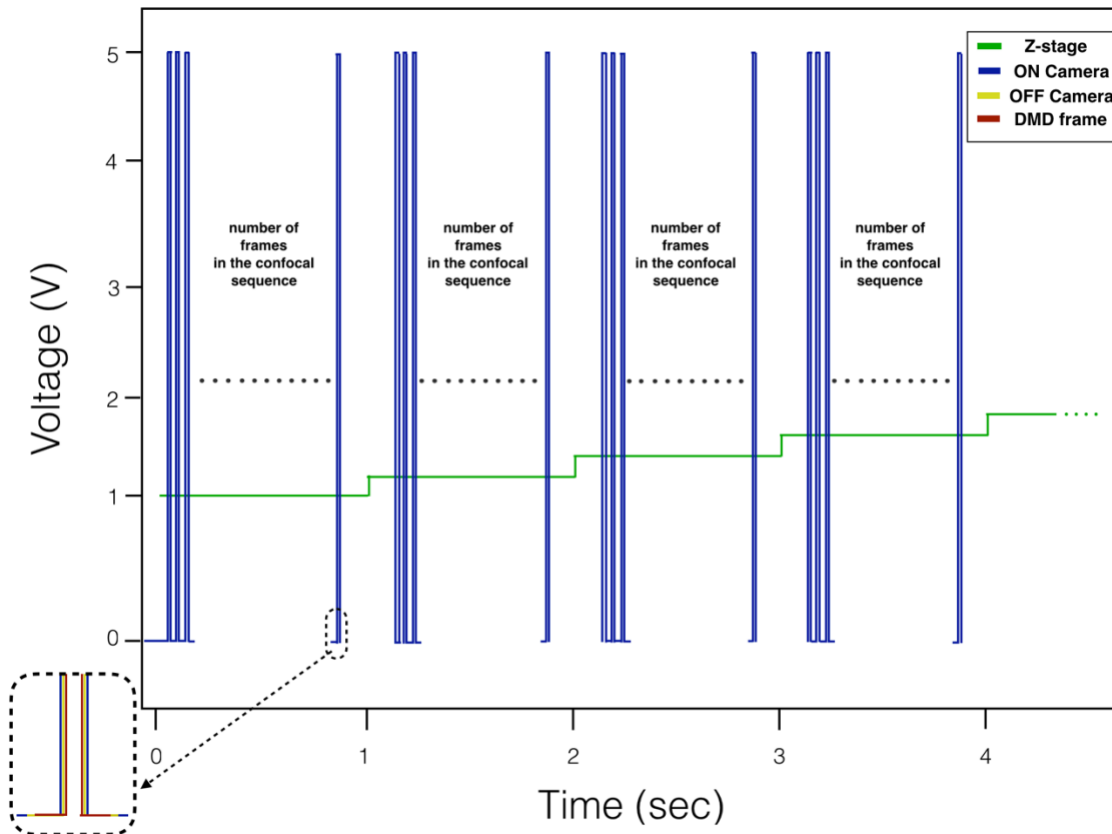
Widefield and rapid confocal images are taken at 10 msec camera exposure time for 1,000 frames on a 100 nm bead sample. As an example, imaging is changed between widefield and confocal randomly using a custom made GUI which is open source with this paper. **Supplementary figure 3(a)** is the first 100 frames in the 1,000 frame sequence summed. **Supplementary figure 3(b)** is frames from 421 to 520 summed. Imaging modalities can be switched between each other in less than 10 msec. Widefield and confocal sequences are pre-loaded on to the DMD onboard memory. 1000 frames are taken as one camera sequence and have the same camera exposure time. For the same camera exposure time, signal-to-noise ratio of confocal is less than widefield because the power delivered to the sample reduces in confocal as only a subset of DMD pixels is ON at a time in a confocal sequence while all the DMD pixels are ON in widefield illumination as can be seen in **supplementary figure 3(c)**.

## Supplementary Figure 4. Control scheme for Z-stage, ON camera, OFF camera, DMD and laser illumination

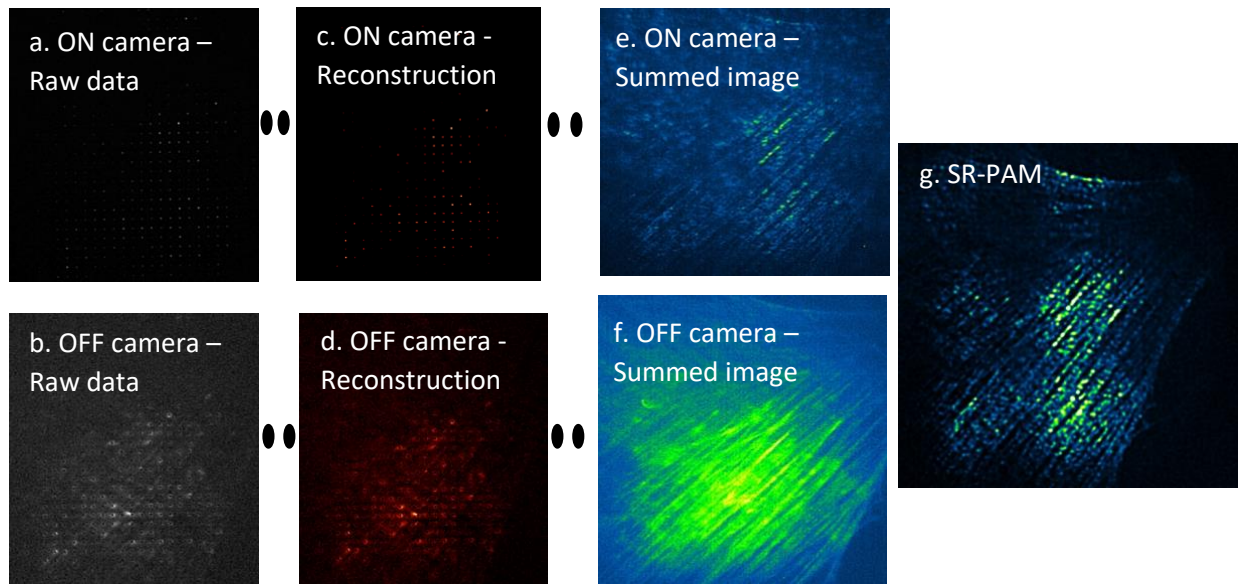
To allow post processing with data from the two cameras, each DMD frame in a confocal sequence needs to be in perfect sync with the corresponding frame of the ON camera and OFF camera. National Instruments DAQ is used to control and synchronize the image acquisition with a custom made LabView program.

Rapid confocal microscopy is configured to achieve the maximum speed by setting the DMD to trigger using an internal timer and is set to 44  $\mu\text{sec}$  per frame which is the minimum reset time for DMD micromirrors. The camera exposure time can be set depending on the sample brightness and desired signal-to-noise ratio of the image. To obtain a z-stack using the rapid confocal modality, the z-stage is controlled externally using a DAQ and the ON camera is run in external exposure mode which is also triggered by the DAQ synchronized to the z-stage movement.

In SR-PAM modality, the NIDAQ is used to trigger z-stage and the ON camera. The ON camera is then used to trigger the OFF camera and the DMD frame change. The DMD in this modality is run in external trigger mode. **Supplementary figure 4** describes the control scheme of image acquisition in rapid confocal and SR-PAM.

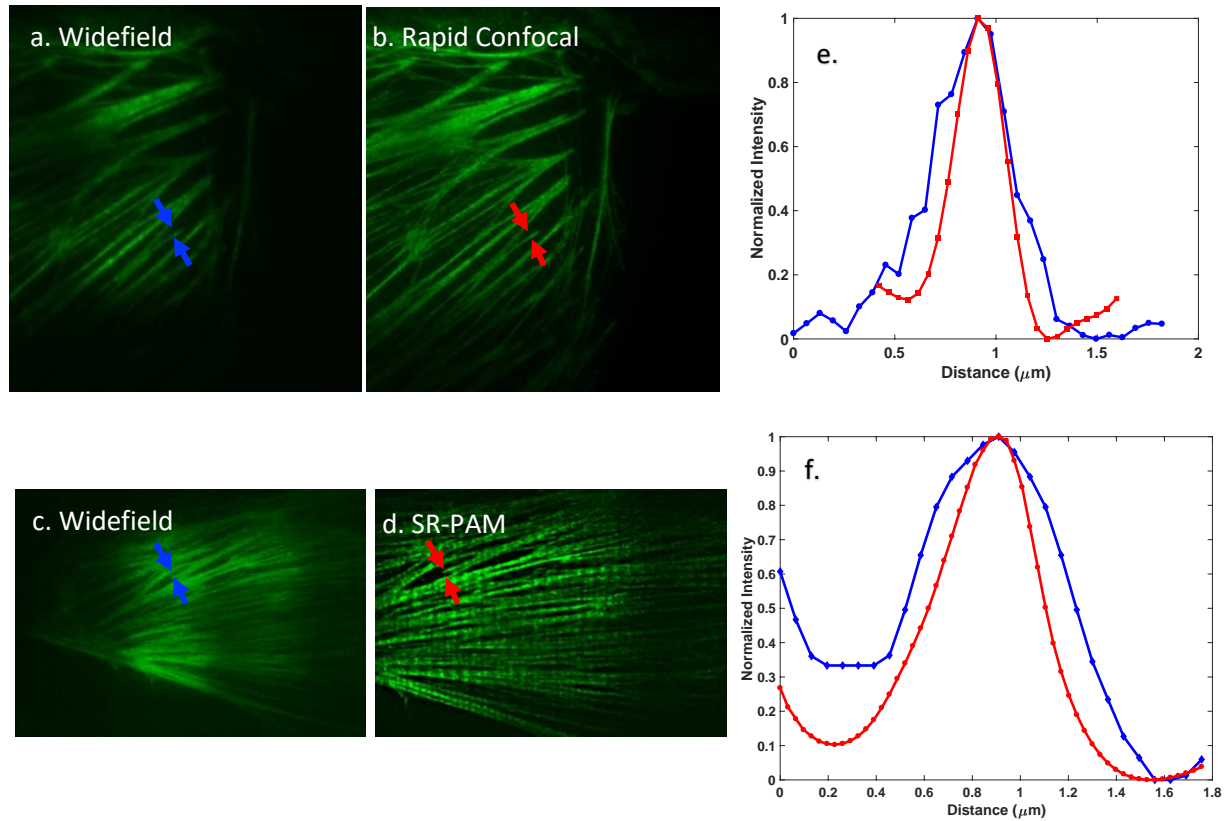


## Supplementary Figure 5. SR-PAM data running in ON and OFF camera on BPAE cells staining for F-actin filaments



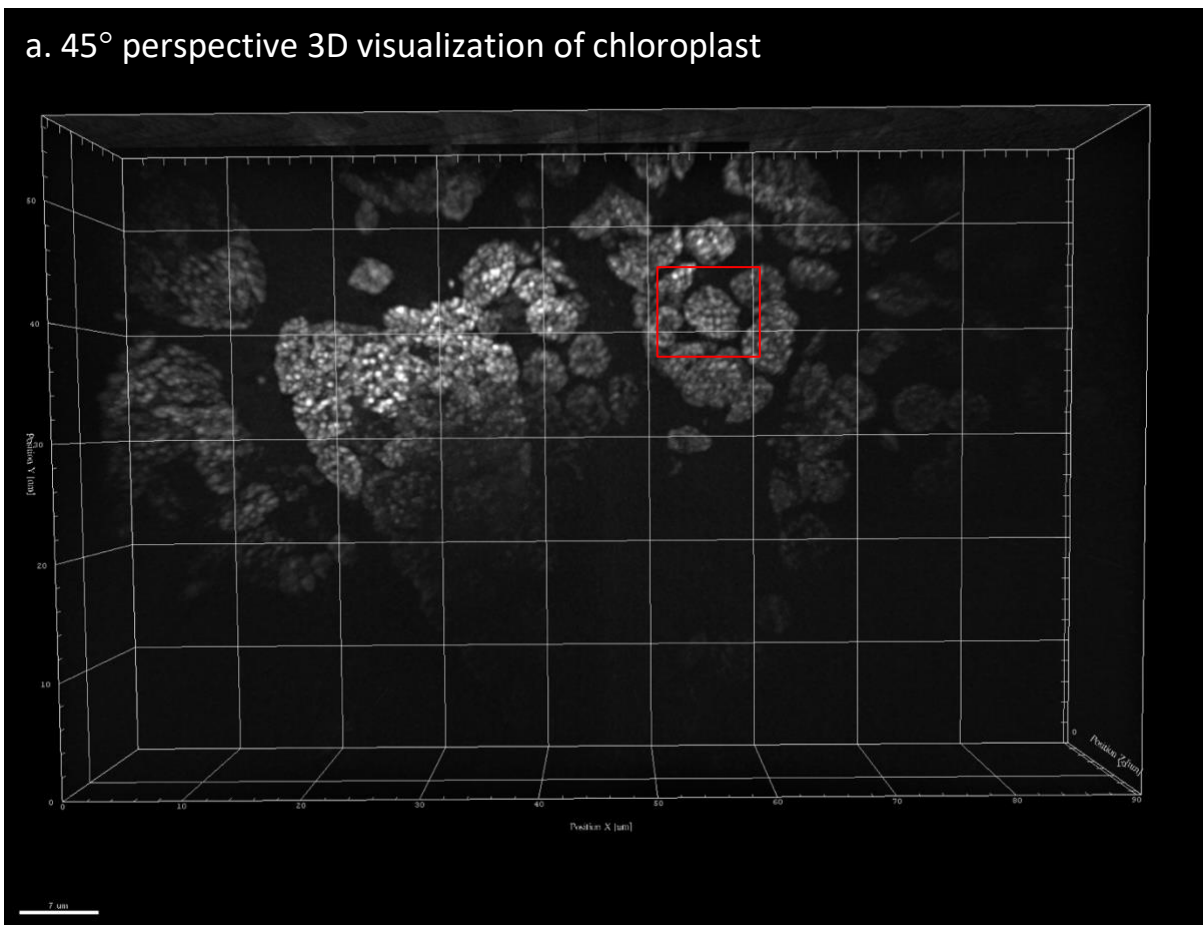
In SR-PAM, the ON camera collects information from in-focus plane of the sample. ON camera data are usually collected in a conventional laser scanning microscope (LSCM) or a spinning disk microscope. The OFF camera collects the data which are usually rejected by a conventional physical pinhole aperture based confocal microscope such as LSCM or spinning disk microscope. Individual multi spot frames collected from the ON and OFF cameras are given in **supplementary videos \* (a) and (b)**. **Supplementary videos \* (c) and (d)** are the simple summed reconstructions in ON and OFF camera respectively. **Supplementary figure 5(e) and 5(f)** are the final summed image for the data collected in ON and OFF camera respectively. **Supplementary figure 5(g)** is the corresponding SR-PAM image which is run through the SR-PAM reconstruction algorithm described in **supplementary note 6** which involves the subtraction of OFF camera PSF from ON camera PSF followed by resolution doubling SR-PAM algorithm.

## Supplementary Figure 6. SR-PAM data running in ON and OFF camera for in BPAE cells staining for F-actin filaments



**Supplementary figure 6(a) and 6(c)** are widefield images. **Supplementary figure 6(b)** is rapid confocal which is running at 227 confocal scans per second. These data are collected at 30 millisecond camera exposure time. If the sample is bright, fast confocal data acquisition is limited only by the maximum speed of the camera mounted in the DMD system. FWHM of the selected actin filament in widefield and rapid confocal in **Supplementary figures 6(a) and 6(b)** are 500 nm and 350 nm respectively as shown in **supplementary figure 6(e)**. **Supplementary figure 6(d)** is an SR-PAM image. FWHM of the selected actin filament of widefield and SR-PAM in **Supplementary figures 6(c) and 6(d)** are 780 nm and 460 nm respectively as shown in **supplementary figure 6(f)**. SR-PAM is obtained with post processing as detailed in **supplementary note 6**. This image can be optionally deconvoluted to enhance the resolution. This resolution improvement can depend on the deconvolution software applied. We used Huygens deconvolution [1] and found that it gave the best resolution improvement. In this **supplementary figure 6**, rapid confocal is reconstructed with Huygens software (classical maximum likelihood estimation) and SR-PAM is reconstructed with AutoQuant (adaptive PSF blind deconvolution).

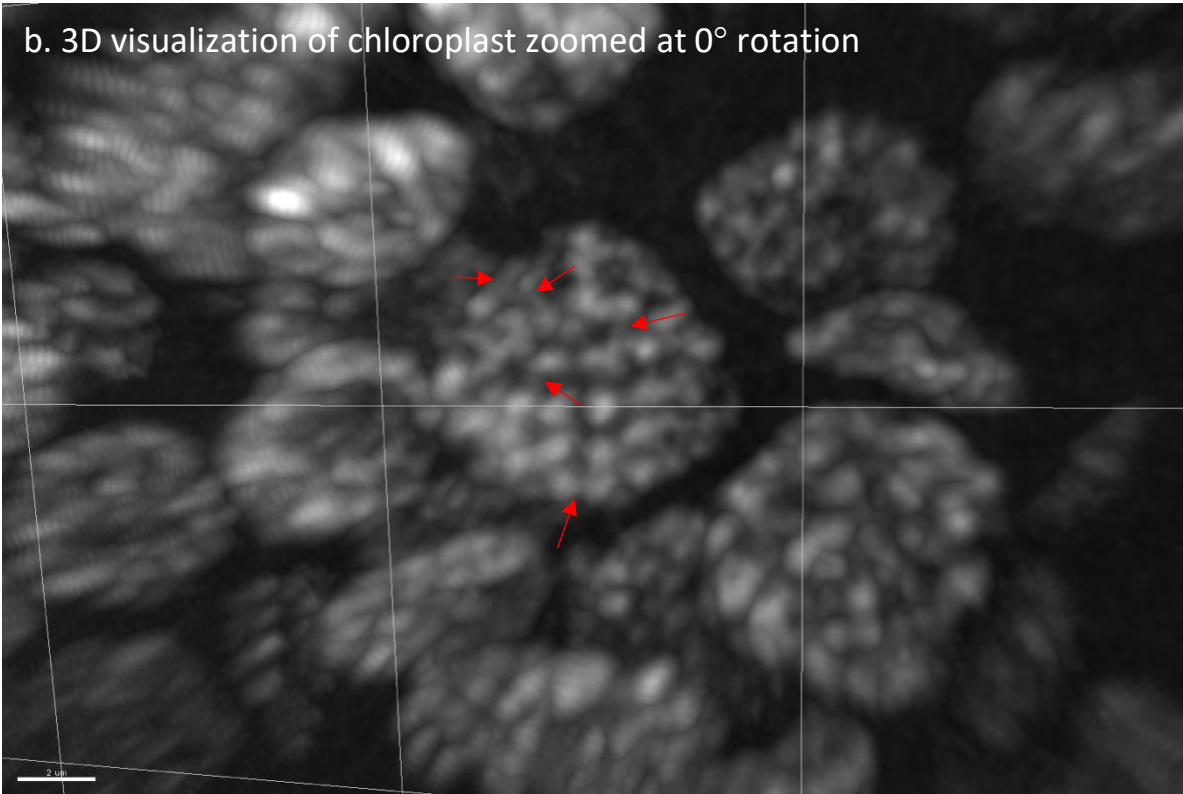
## Supplementary Figure 7. Visualization of Stromal Lamella in Plant Chloroplast



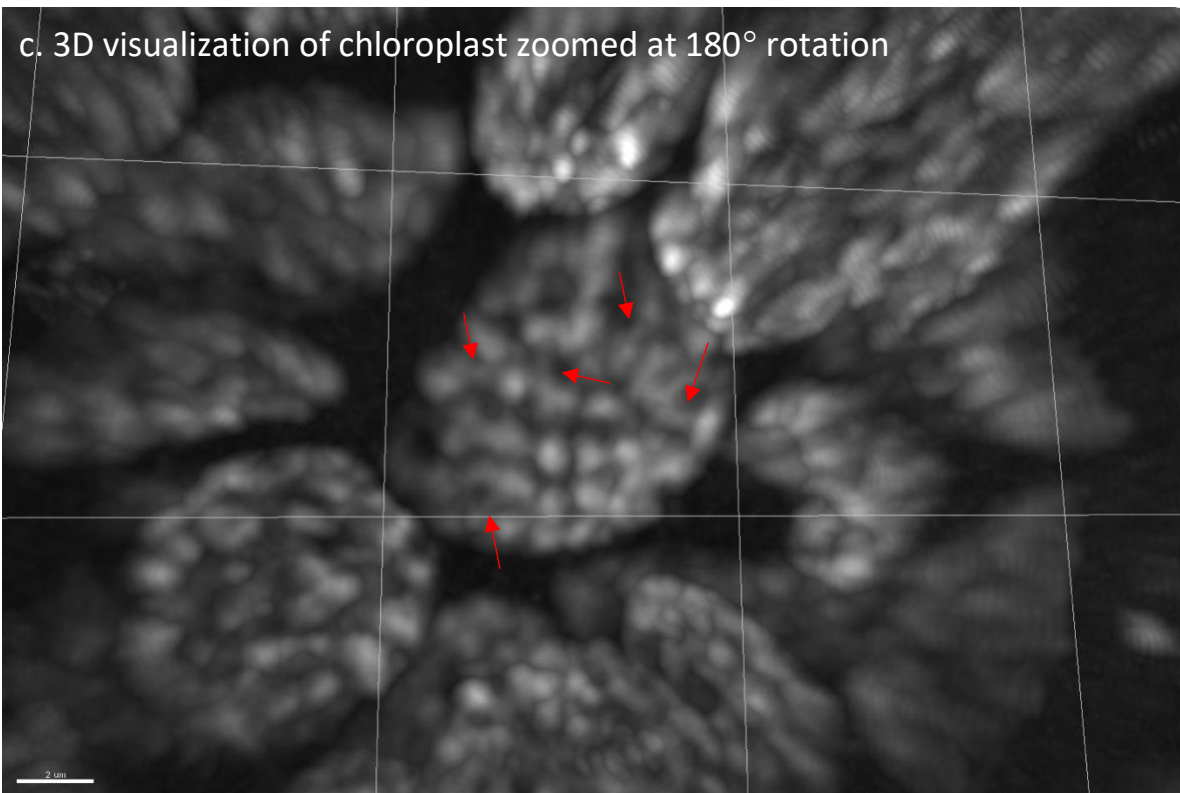
**Supplementary figure 7(a)** is a 45° perspective of 3D visualization of chloroplasts in a spinach leaf tissue. **Supplementary video 6** shows the complete z-stack of the chloroplasts organized in the tissue. **Supplementary figures 7(b)** and **7(c)** are snapshots from the video at 0° and 180° rotations respectively. Red arrows indicate the location of stromal lamellae which are links between the grana. These diffraction limited structures are only a few nanometres thick as visualized in electron microscopes previously. Due to their size and location it has been extremely difficult to visualize these with SIM which has limited axial depth and conventional confocal which is limited by deep imaging and resolution. **Supplementary figure 7(d)** is the z-axis slices of the chloroplasts selected with red square in **Supplementary figure 7(a)**. Although the structure has been seen with electron microscopes previously, we report the precise localization of these structures achieved with optical microscopy.



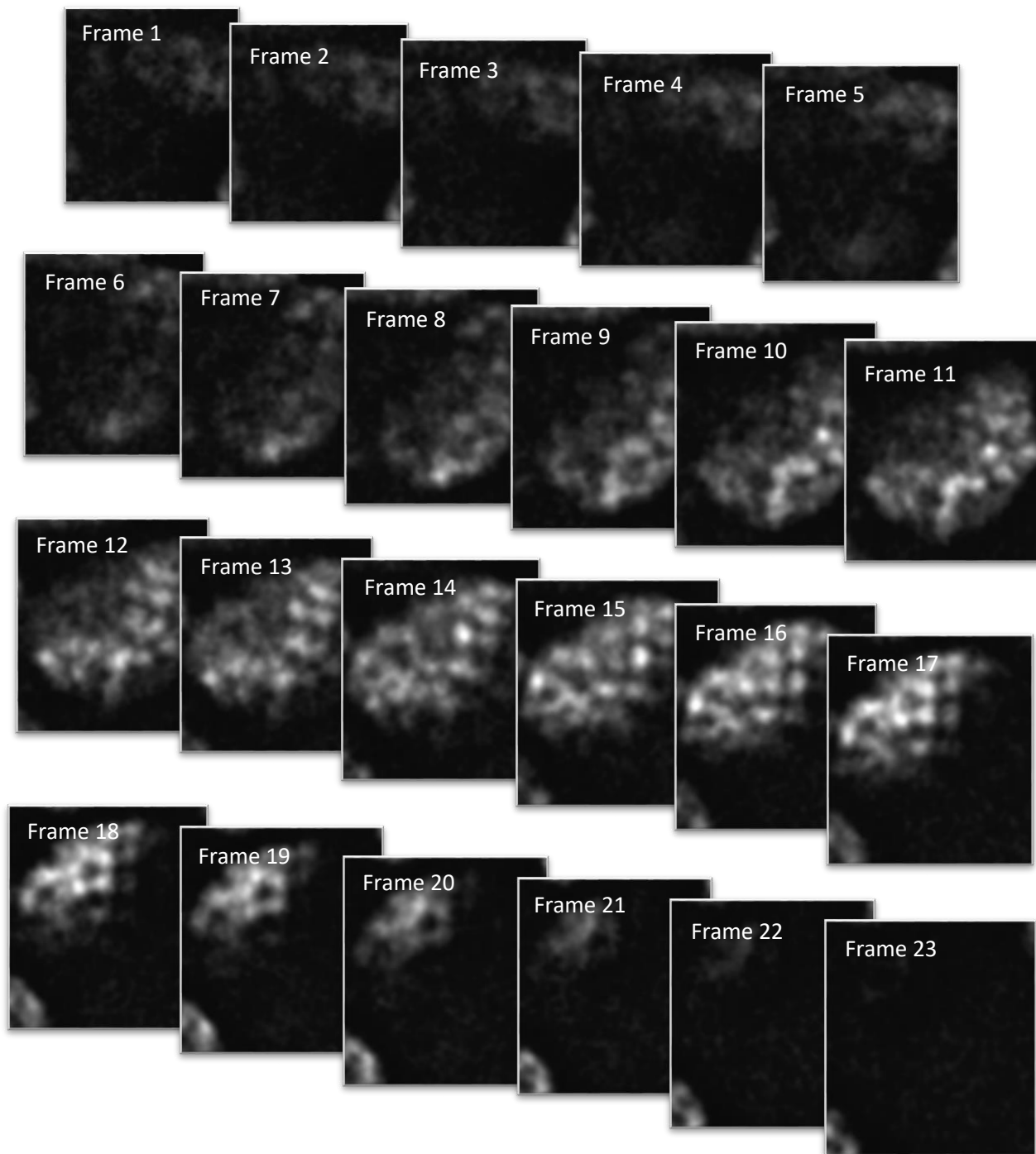
b. 3D visualization of chloroplast zoomed at 0° rotation



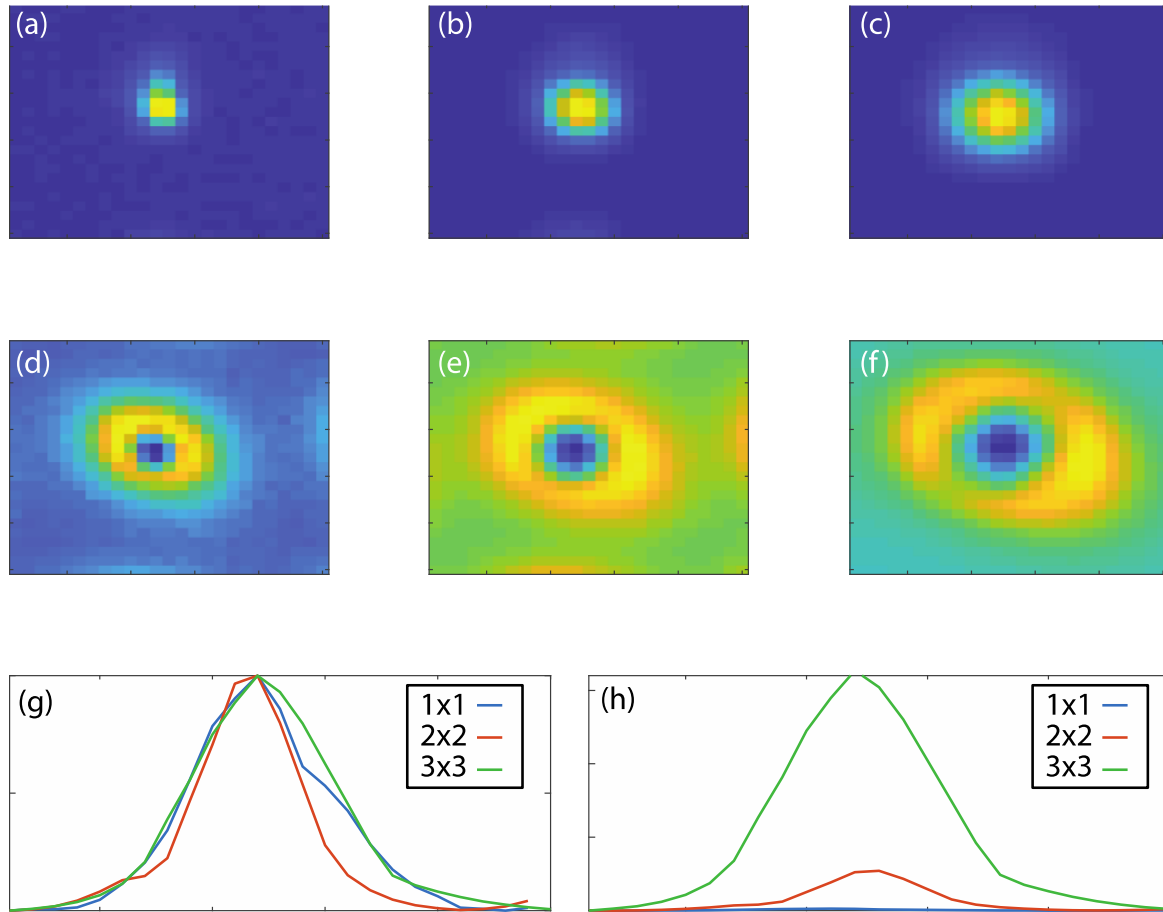
c. 3D visualization of chloroplast zoomed at 180° rotation



d. 23 axial slices through one chloroplast

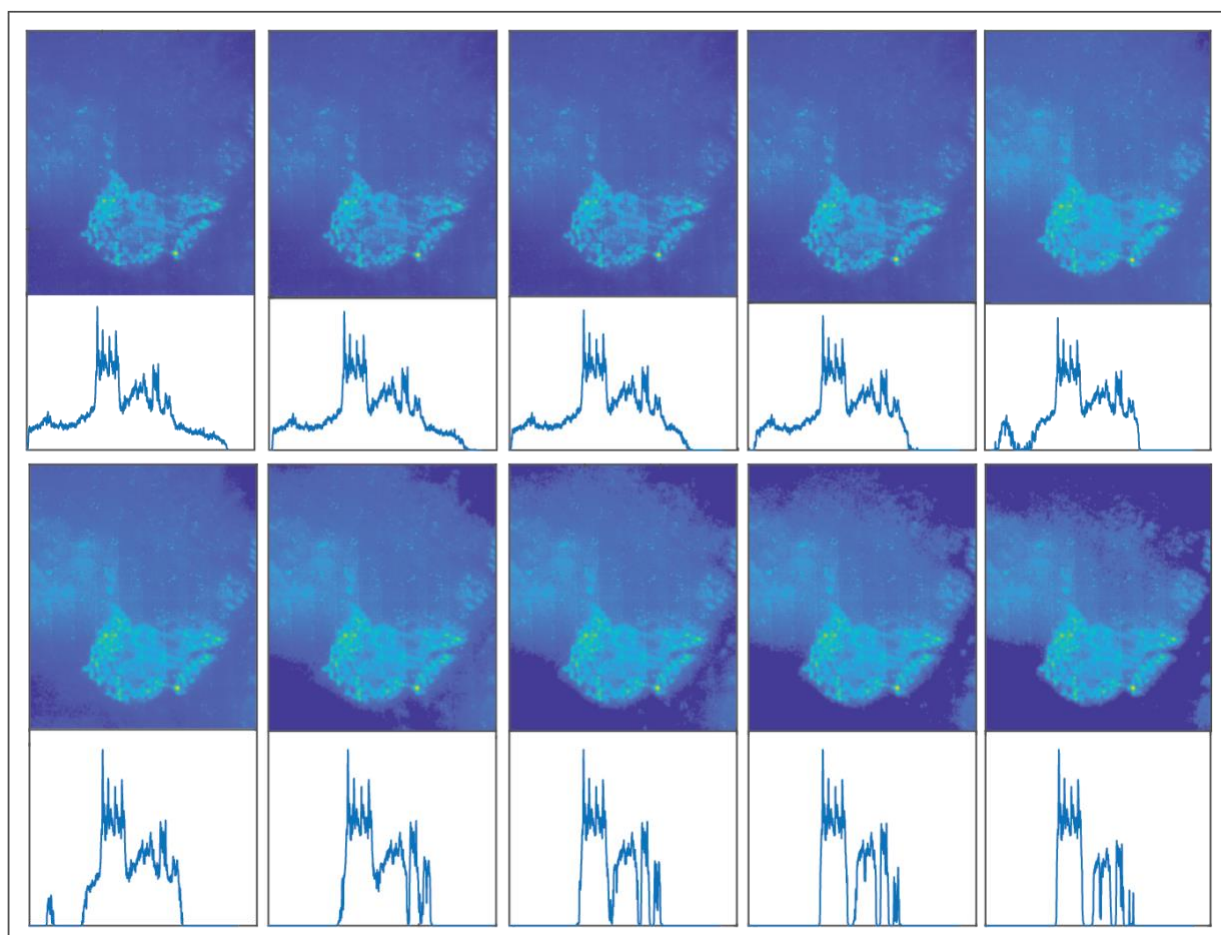


### Supplementary Figure 8. ON and OFF PSF of various pinhole size



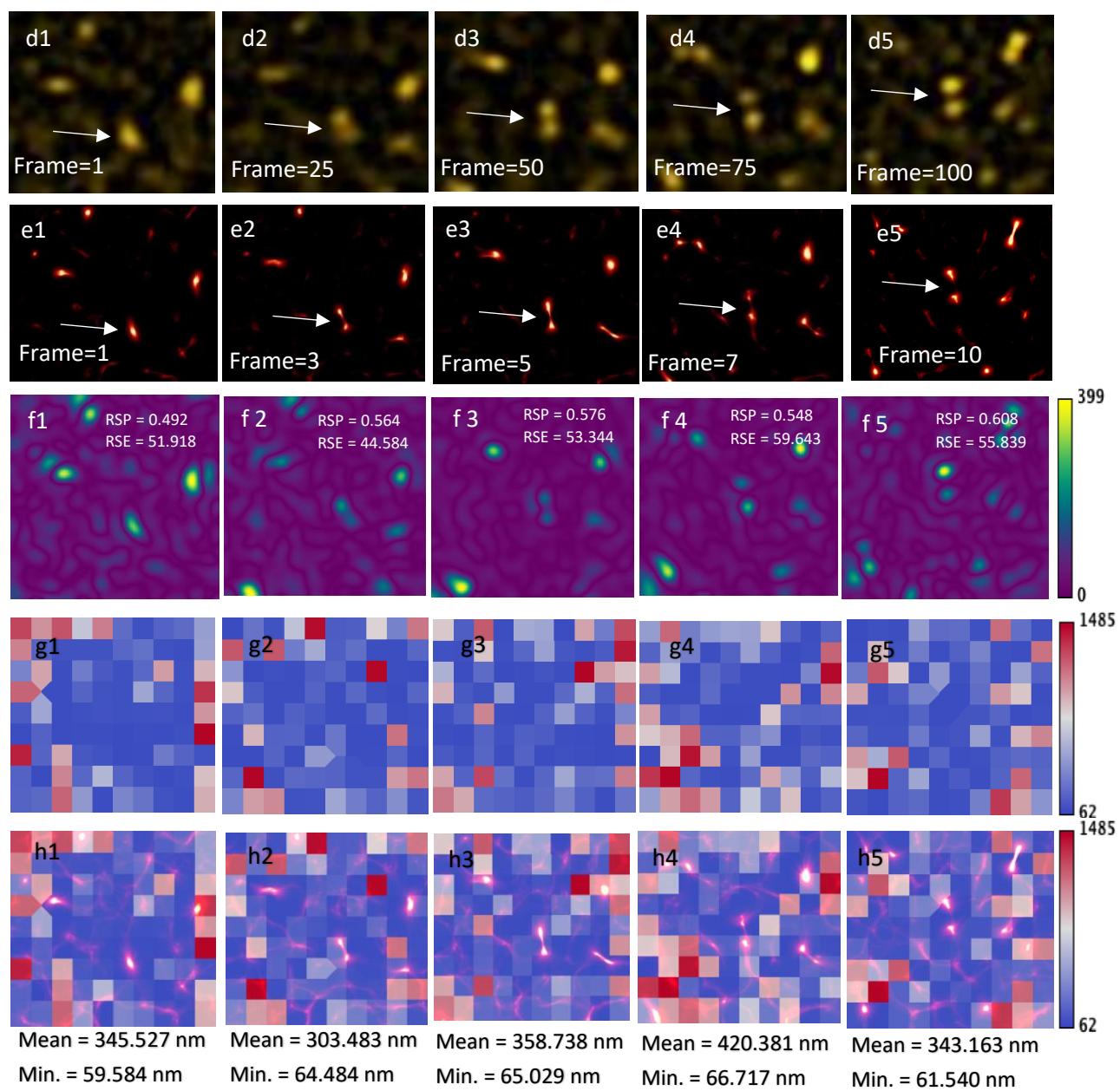
SI Figure 8. The collected point spread function (collected on the ON camera) parts a – c and the reject point spread function (collected on the OFF camera) parts d – f. Parts a and d were for 1 DMD pixel, corresponding to an effective pinhole size of 130 nm (1 DMD pixel) at the image place. Parts b and e represent a pinhole size of 260 nm (2 DMD pixels) while parts c and f represent 390 nm (3 DMD pixels). A normalised line profile for the three pinhole sizes, 1x1, 2x2 and 3x3 DMD pixels is given in part g while the un-normalised line profile is given in h, the 1x1 DMD pixel pinhole has a greatly reduced intensity,

## Supplementary Figure 9. Threshold



SI Figure 9. ISM data as a function of threshold. The XXX algorithm require the confocal spots to be identified by an initial localisation step using a localisation microscopy program such as RapidStorm or ThunderStorm. This require a detection threshold; the figures above have been reconstructed with varying threshold values using Thunderstorm. Top left has a threshold value set to twice the noise value, each image has double the threshold until the bottle right image which has a threshold of twenty times background.

**Supplementary Figure 10. SQUIRREL analysis of centrosome figure 1**



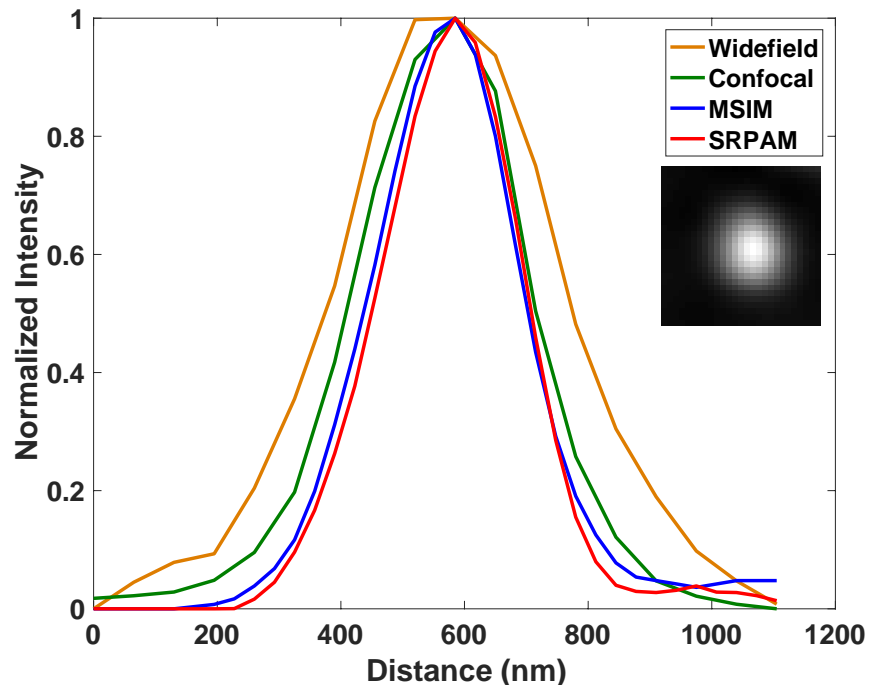
**Supplementary figure 10** shows the SQUIRREL [2] analysis of mitotic division of centrosomes in **figure 1**. **Supplementary figures (f1-f5)** show the error maps with reference frames as **d1-d5** and super resolution frames as **e1-e5**. **Supplementary figures (g1-g5)** show the FRC maps between **d1-d5** and **e1-e5**. **Supplementary figures (h1-h5)** show the overlay between **e1-e5** and **g1-g5**.

### **Supplementary Note 1. Resolution calibration of SR-PAM and comparison with other point based illumination techniques.**

Fluorescent beads of 100 nm were used to calibrate the resolution of SR-PAM and it was compared with other point illumination based imaging techniques. A widefield image was obtained with all the DMD pixels ON. Confocal image was acquired with 2x2 DMD pixel pinhole size (272 nm in image space) and inter pinhole distance 2x5 DMD pixels (1,360 nm in image space). These confocal data were acquired in rapid mode without deconvolution. SR-PAM data were acquired using both ON and OFF camera with the same pattern as used for acquiring rapid confocal image. SR-PAM was reconstructed with the post processing algorithm (**supplementary note 6**). Image acquired after running the data through the post processing algorithm of SR-PAM was not deconvoluted for this bead data to demonstrate the resolution improvement of the technique even without deconvolution.

MSIM image is reconstructed using the SR-PAM raw data. The original MSIM optical set up does not use a physical pinhole to reject the out-of-focus intensity, but it uses a digital pin holing process by multiplying the emission spot with a Gaussian mask of SD 1.5. In SR-PAM set up, emission spots acquired in ON and OFF camera were added to restore the full emission spot without any physical out-of-focus rejection, equivalent to MSIM optical set up. The spot is multiplied by a Gaussian mask of SD 1.5 followed by ISM procedure to enhance the resolution and acquire the MISIM equivalent image using SR-PAM set up.

**Supplementary note 1 figure** represents the normalized intensity plotted against distance for widefield, confocal, MSIM, and SR-PAM of 100 nm bead sample. **Inset** is the image of 100 nm bead SR-PAM image. FWHM of widefield is 400 nm, confocal is 317 nm, MSIM is 270 nm and SR-PAM is 261 nm. SR-PAM without deconvolution provides a resolution improvement of more than  $\sqrt{2}$ . This is attributed to the additional out-of-focus subtraction. Deconvolution further enhances the resolution. It is to be noted that none of the images in this section is deconvolved. This is to acquire and compare the resolution improvement of techniques without deconvolution and to demonstrate the resolution improvement of SR-PAM.



## Supplementary Note 2. Theory of SR-PAM

The theory of SR-PAM is derived as an extension of PAM and ISM interpretations pioneered by Jovin Thomas in around 1990s and Sheppard in around 1980s respectively. A PAM system is based on patterned illumination projection and patterned emission collection positioned in the same physical location, the SLM plane. The major advantage here is that the excitation and collection planes coincide in such a way that there are no alignment issues. Conventional PAM system has found its applications in FRET and conventional confocal microscopy. In the conventional PAM system, image collected in the ON camera is interpreted as an ‘analog of a confocal image’ as it is without processing. Considering the simulations in **supplementary note 3**, we obtain the raw data for SR-PAM by doing a weighted subtraction of the data collected in ON and OFF images to subtract the intensity bleed through from out-of-focus planes of the sample. We achieve this with the collection and mapping of each illumination and emission spots to give

high level control enabling superior out-of-focus light subtraction and the ability to do other point-based illumination techniques detailed in **supplementary note 4**.

When imaging a sample in a microscope with uniform widefield illumination, image formed on the detector is a convolution of the sample and the excitation PSF of the microscope. Expression for the image formed at the detector is given by,

$$I_w = \int \text{Hem} (xc - u, yc - v, w) S (u, v, w) du dv dw \quad (1)$$

where, Hem is the PSF formed on the camera (camera coordinates represented by xc, yc), if there is a point detector at position (u, v, w) in the sample S.

When using patterned projection, image formed in the camera is modified with respect to the illumination pattern. Here, an illumination pattern G is projected on to the DMD plane and de-magnified on to the sample plane with a magnification factor M. Modulation pattern we use is a multiple square pattern shown in **supplementary note 5**. Image is collected on the DMD. ON pixels reflect light on to the ON camera and OFF pixels reflect light on to the OFF camera. In-focus or conjugate image is formed in the ON camera and out-of-focus or non-conjugate image is formed on OFF camera. Here we consider DMD coordinates (xd, yd) as the detector coordinates. Conjugate image is given by,

$$I_{c, G} (x_d, y_d, z_s) = \frac{T}{n_x n_y} \iiint_{-\infty}^{+\infty} \text{Hem} \left( \frac{x_d}{M} - u, \frac{y_d}{M} - v, w \right) \quad (2)$$

$$* I_G \left( u - \frac{x_d - \phi_x}{M}, v - \frac{y_d - \phi_y}{M}, w \right) * S (u, v, w - z_s) du dv dw$$

where, Hem is the emission PSF,  $\phi_x, \phi_y$  is defined as  $x_d, y_d \bmod \eta$ ,  $\eta$  is the size of the DMD pixel,  $z_s$  is the axial direction depth of field, T is the total integration time and S is the density function of the emitter.  $I_G$  is the total illumination function given by,

$$I_G (x_o, y_o, z_o) = \iint_{-\infty}^{+\infty} G (Mu, Mv) * \text{Hex} (x_o - u, y_o - v, z_o) du dv \quad (3)$$

where G is the modulation pattern defined by equation (4) and follows the condition (5),

$$G (x_d, y_d) = G (x_d - pn_x \eta, y_d - pn_y \eta) \quad p, q \in \mathbb{N} \quad (4)$$

$$\sum_{a=0}^{n_x-1} \sum_{b=0}^{n_y-1} G (x_d - a\eta, y_d - b\eta) = 1 \quad (5)$$



where, (nx, ny) are the number of columns and rows in the DMD and ‘a’ and ‘b’ are pixel numbers with limits  $0 \leq a \leq nx$  and  $0 \leq b \leq ny$ .

The non-conjugate image is given by substituting modulation pattern G by 1-G,

$$G_{nc}(Mu, Mv) = 1 - G(Mu, Mv) \quad (6)$$

Substituting equation (6) and equation (3) in equation (2) gives the non-conjugate image as,

$$I_{nc, G}(x_d, y_d, z_s) = \frac{T}{n_x n_y} \iiint_{-\infty}^{+\infty} \text{Hem}\left(\frac{x_d}{M} - u, \frac{y_d}{M} - v, w\right) \\ * (1 - G(Mu, Mv)) * \text{Hex}(u, v, w) * S(u, v, w - z_s) du dv dw \quad (7)$$

For obtaining the SR-PAM image, we subtract the bleed through of out-of-focus intensity of each emission spot on the conjugate image by using the non-conjugate image followed by pixel reassignment to increase the resolution of the image by  $\sqrt{2}$ . We can deconvolve this image with the ‘real’ point spread function to obtain the final image. By ‘real’ PSF we mean that we need not rely on the theoretical PSF or calibrated PSF (generally calibrated using beads), we can obtain the ‘real’ PSF from the image by doing,

$$\text{PSF}_{\text{real}} = \text{PSF}_{\text{ON}} - \text{invert}(\text{PSF}_{\text{OFF}}) / \Phi \quad (8)$$

where  $\Phi$  is the scaling constant which can be varied depending on the thickness of the sample. Value of  $\Phi$  used here is 10 which is modelled in **supplementary note 3**. Before pixel reassignment, the raw SR-PAM data are given by the equation,

$$\text{Raw } I_{\text{SR-PAM}} = I_c - I_{nc} / \Phi \quad (9)$$

Substituting (2) and (7) in equation (9) we get,

$$\text{Raw } I_{\text{SR-PAM}}(x_d, y_d, z_s) = \frac{T}{10 * n_x n_y} \iiint_{-\infty}^{+\infty} \text{Hem}\left(\frac{x_d}{M} - u, \frac{y_d}{M} - v, w\right) \\ * (11 * G(Mu, Mv) - 1) * \text{Hex}(u, v, w) \\ * S(u, v, w - z_s) du dv dw \quad (10)$$

New  $I_G$  for the raw  $I_{\text{SR-PAM}}$  can be given as,

$$I_{\text{Gnew}}(x_o, y_o, z_o) = \iint_{-\infty}^{+\infty} (11 * G(Mu, Mv) - 1) * \text{Hex}(x_o - u, y_o - v, z_o) du dv \quad (11)$$

and raw  $I_{\text{SR-PAM}}$  can be derived as,

$$\text{Raw } I_{\text{SR-PAM}}(x_d, y_d, z_s) = \frac{T}{10 \cdot n_x n_y} \iiint_{-\infty}^{+\infty} \text{Hem} \left( \frac{x_d}{M} - u, \frac{y_d}{M} - v, w \right) \\ * I_{\text{Gnew}} \left( u - \frac{x_d - \phi_x}{M}, v - \frac{y_d - \phi_y}{M}, w \right) * S(u, v, w - z_s) du dv dw \quad (12)$$

We can simplify this by setting DMD coordinates  $(x_d, y_d, z_s)$  to  $\mathbf{s}$  and sample coordinates  $(u, v, w)$  to  $\mathbf{r}'$ . Raw SR-PAM image can be obtained by integrating the above equation (12) with  $x_d$  and  $y_d$  (or  $\mathbf{s}$ ).

$$\text{Raw } I_{\text{SR-PAM}}(\mathbf{r}, \mathbf{s}) = \iint \text{Hem}(\mathbf{s} - \mathbf{r}' + \mathbf{r}) * I_{\text{Gnew}}(\mathbf{r} - \mathbf{r}' - f(\mathbf{s})) * S(\mathbf{r}') ds dr' \quad (13)$$

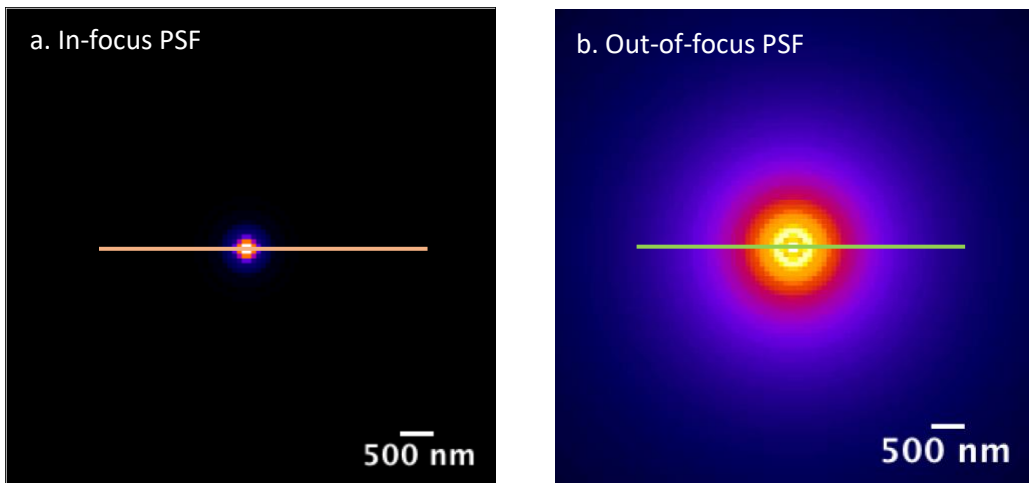
where  $f(\mathbf{s})$  is a function of  $\mathbf{s}$  defined by substituting  $\mathbf{s}$  for  $x_d$  in  $\frac{x_d - \phi_x}{M}$ . Each pixel in the DMD is considered as an independent detector. Raw SR-PAM image is processed by pixel reassignment to increase the resolution. Pixel reassignment shifts the displaced pinhole by half the distance towards the optical axis. Thus SR-PAM image can be represented as,

$$I_{\text{SR-PAM}}(\mathbf{r}, \mathbf{s}) = \iint \text{Hem} \left( \frac{\mathbf{s}}{2} - \mathbf{r}' + \mathbf{r} \right) * I_{\text{Gnew}} \left( \mathbf{r} - \mathbf{r}' - f(\mathbf{s}) - \frac{\mathbf{s}}{2} \right) * S(\mathbf{r}') ds dr' \quad (14)$$

Function  $f(\mathbf{s})$  in the excitation PSF represents the pinholes in excitation pathway projecting the intensity spot and in emission pathway collecting the intensity spot. The effective PSF of SR-PAM system can be written as,

$$\text{PSF}_{\text{SR-PAM}}(\mathbf{r}) = \int \text{Hem} \left( \frac{\mathbf{s}}{2} + \mathbf{r} \right) * I_{\text{Gnew}} \left( \mathbf{r} - f(\mathbf{s}) - \frac{\mathbf{s}}{2} \right) ds \quad (15)$$

### Supplementary Note 3. Simulation



When collecting a confocal image with any type of physical apertures, there is an intensity bleed through from out-of-focus planes in the in-focus camera. We simulated a PSF using Born and Wolf 3D Optical Model (we used PSF generator in ImageJ plugin) to estimate the weighing factor for the subtraction of non-conjugate image from conjugate image. PSF of in-focus (**supplementary note 3 figure (a)**) and out-of-focus (**supplementary note 3 figure (b)**) pixel PSF is calculated with pixel size in x,y as the size of the camera pixel 65 nm, z step as 300 nm, N.A 1.4 and refractive index 1.5. Estimated depth of field (which is higher than the axial resolution due to diffraction limited optics) for 100x 1.45 oil objective as 500 nm. **Supplementary note 3 figure (c)** is the intensity profile of the in-focus and out-of-focus PSF. The black arrow in **supplementary note 3 figure (c)** indicates the bleed through intensity from out-of-focus planes in the in-focus image. The contribution of ‘1/10’ out-of-focus intensity to the final SR-PAM raw data comes from here. It is to be noted that this intensity profile should not be confused with the actual intensity of emission light from in-focus and out-of-focus planes collected in both the cameras. Intensity of out-of-focus light for moderately thick sample is several times higher than light collected from the in-focus plane. It has been shown that almost 90% of emission light from the sample in an optical microscope is from planes above and below the focal plane. A quantitative measurement of this with varying pinhole sizes in a point based illumination system is given in **supplementary figure 8**.

## **Supplementary Note 4. DMD-dual camera calibration**

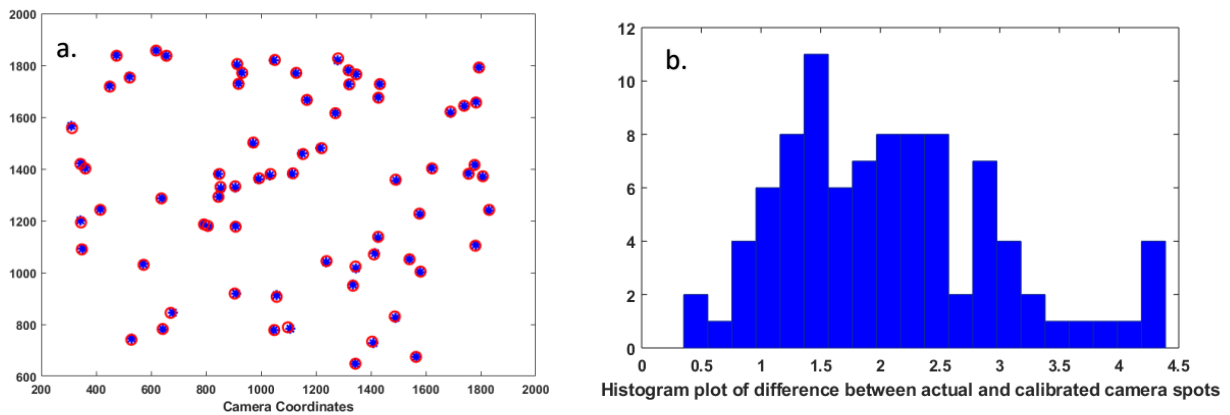
### **Primary Calibration**

Post processing for SR-PAM which involves subtraction of out-of-focus OFF camera data from in-focus ON camera data, requires precise mapping of each DMD pixel to its corresponding camera pixel in camera A and camera B. For taking calibration data, DMD can either be back illuminated through the microscope with a bright light source without the objective in place or a flat fluorescent sample can be used instead. The following procedure is followed for primary calibration,

1. Primary calibration is done by collecting N frames with one random but known DMD pixel ON per frame. The corresponding image stack is collected in camera ON and camera OFF.

2. The known DMD and camera points from the above data are used to find the translation vector to translate all the pixels in DMD plane to the corresponding pixels in camera plane.
3. To decrease the error of mapping, a rotation component is added to the translation vector. Expected DMD pixels calculated from the translation vector are rotated to find the angle of rotation which gives minimum separation between expected and actual camera spots.
4. This angle of rotation which gives the minimum deviation of expected camera spots from actual camera spots is recorded and used to rotate all the expected camera spots with this angle to give the new expected camera spots.

**Supplementary note 4 figure (a)** plots a projection of all 100 frames collected using the above method with one DMD pixel ON in each frame. Blue (\*) and red (o) denote expected camera points and actual camera points respectively. **Supplementary note 4 figure (b)** is a histogram plot of difference between expected camera points and actual camera points. There is less than 100 pixels deviation in calibration for the primary calibration method.

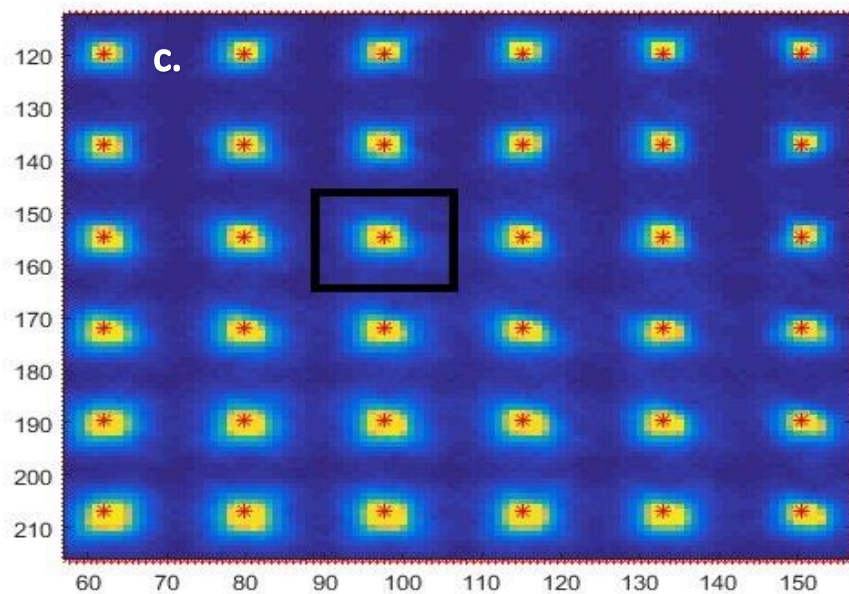


**Supplementary note 4 fig. Calibration.** (a) Plot of N=100 frames with one pixel ON in each frame. (b) Histogram plot of difference between actual and calibrated camera spots in camera coordinates.

### Secondary Calibration

Non-linear deviation of the expected DMD pixels from the actual camera points and the requirement of the mapping precision to be less than a diffraction limited spot, call for a secondary calibration. This is achieved by collecting 100 frames of 1x1 ON pixels with 10 pixels apart multifocal patterns scanned across the DMD. These data are collected for both camera ON and camera OFF. For each DMD pixel in the known multifocal pattern, expected spot positions in camera are calibrated using the primary calibration method as described above. For each illumination spot in the camera, a square area is cut out around this expected camera spot in the multifocal camera data as shown in **supplementary note 4 figure (c)**. The pixel corresponding to the maximum intensity in the cut out square area is saved as the exact camera spot when that

particular DMD pixel is illuminated. These exact illumination spots are recorded and saved for all the 1024x768 DMD pixels for both cameras separately. This gives a calibration precision with a maximum deviation of not more than two camera pixels equivalent to 1 DMD pixel) in an Andor sCMOS zyla 4.2 camera which is equivalent to less than 130 nm in sample coordinate with a 100x objective. These are saved for further post processing applications.

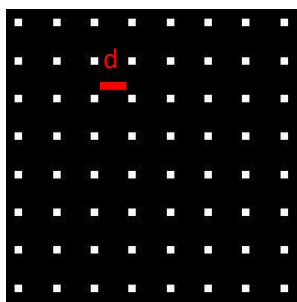


**Supplementary note 4 fig. (c)** Actual illumination spots are yellow and expected illumination spots marked in asterisks.

## Supplementary Note 5. Modulation Pattern and Rapid Confocal Post Processing

The SR-PAM illumination pattern is a square grid of ON and OFF pixels as shown in **supplementary note 5 figure**. The distance  $d$  between two adjacent pixels can ideally vary from 8 to 12 DMD pixels depending on which, the number of frames needed for reconstruction also varies. If the pinholes are close, there will be increased cross talk between the pixels and will decrease the optical sectioning ability of the system. If the pinholes are far apart, it will increase the number of frames required for reconstruction decreasing the speed of imaging. To illuminate the whole area of one frame, this pattern is repeated  $d^2$  times and the image is recorded on the camera. The size of the pinhole of a confocal pattern can be changed by changing the number of

ON pixels in the DMD as 1x1, 2x2, 3x3 and so on. Abbe diffraction limited spot size for 488 nm illumination light source is in theory  $\lambda/2NA = 168$  nm. Each DMD pixel size is  $13.6 \mu\text{m} \times 13.6 \mu\text{m}$  and a 100x/1.49 NA objective is used for imaging. Ignoring the diffraction limit, one DMD pixel should illuminate  $136 \text{ nm} \times 136 \text{ nm}$  area of the sample. We find that using 2x2 or 3x3 ON pixels in square grid pattern gives the optimal signal-to-noise ratio and optical sectioning of the sample. A 2x2 and 3x3 pixels DMD spot theoretically illuminates  $272 \text{ nm} \times 272 \text{ nm}$  and  $408 \text{ nm} \times 408 \text{ nm}$  in sample plane respectively.



(Supplementary note 5 fig. SR-PAM illumination pattern)

As described previously, the patterned illumination presented in the paper has two major modes of operation which can be switched depending of the sample and the biological investigation. Rapid confocal can potentially run at 355.11 confocal scans/second enabling rapid live biological imaging. In rapid confocal, out-of-focus light from the plane above and below the focal plane is rejected physically by micro-mirrors. Each in-focus camera frame collects several complete confocal images by summing each pinhole intensity for all the frames of several confocal scans in one camera frame. The final image can be deconvoluted to restore the resolution. This image can be run through super resolution reconstruction algorithms to enhance the resolution. In this paper we use SRRF reconstruction [3].

## Supplementary Note 6. SR-PAM post processing

Confocal based structured illumination microscopy imaging, SR-PAM, described in this paper with post processing collects the in-focus and out-of-focus PSF separately to make the most efficient use of the fluorescence emission from the sample. SR-PAM is slow compared to rapid confocal as there is a need to collect all the illumination frames of confocal ON and OFF data in two separate cameras frame by frame and then running the data through the reconstruction code to get a weighed subtraction of out-of-focus plane emission intensities from in-focus plane intensities to drastically improve the signal-to-noise ratio.

Point illumination based techniques use either a physical pinhole or a digital pinhole to reject the out-of-focus light. A physical pinhole is a physical aperture to block the out-of-focus light such as in conventional laser scanning microscope, spinning disk microscope etc. This can reduce the intensity of the signal collected because the aperture blocks a major part of the emission intensity. In digital pin holing, the emission spot is fitted to a Gaussian mask. As out-of-focus light change throughout the sample as the structures in biological samples are highly inhomogeneous. In SR-PAM out-of-focus subtraction is advanced in this regard as it is solely optical with no requirement of digital pin holing or the assumption of out-of-focus PSF being constant throughout the sample.

Raw data are collected using either 3x3 pin holing with 225 frames or 2x2 pin holing with 100 frames in ON camera and OFF camera. The ON and OFF data are run through the reconstruction code. Following are the main steps involved in reconstruction,

1. In the code, we go to each DMD illumination spot one by one and find the position of each spot in the ON and OFF camera data using the calibration lookup table found using the camera-DMD calibrating technique detailed in **supplementary note 5**.
2. We cut a square area around each illumination spot in all the frames. These cut sections are saved for ON and OFF data separately. This increases the versatility of the system with the ability to build the final image using various modalities with post processing.
3. Divide the OFF data by 10 and subtract this with ON data.
4. Magnify this cut section with a magnifying factor (We use mag=8). Build a zero matrix with size equal to  $2 * \text{mag} * \text{number of pixels in camera}$ . Add the cut sections back to this matrix and magnify the matrix by a magnifying factor.
5. Deconvolve the matrix obtained in step 2 image.

Optionally, we can mask the square cut section around the subtracted cut section obtained in step 3. This can improve the signal-to-noise ratio of thick samples.

## **Supplementary Note 7. AiryScan equivalent algorithm using a camera based optical setup: AiryImaging**

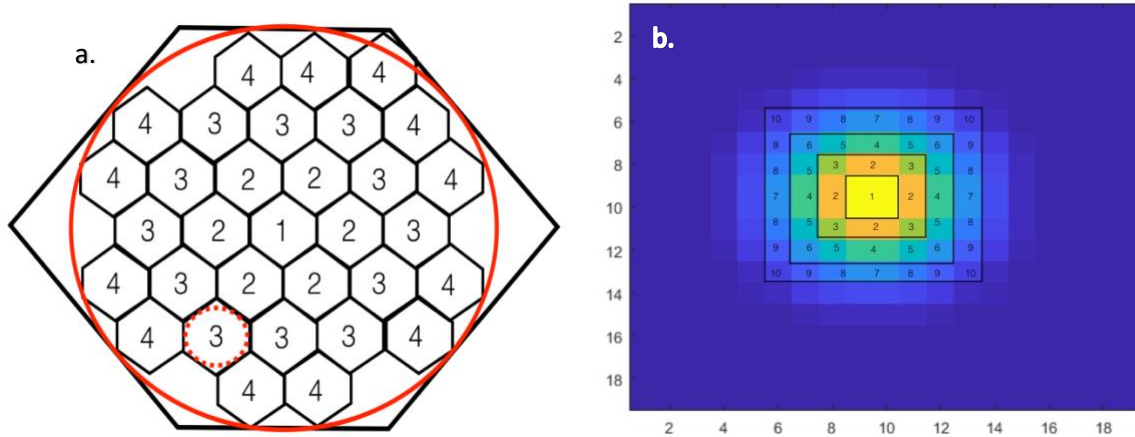
This section details a method and algorithm to obtain an AiryScan image equivalent using any camera based confocal set up. Image Scanning Microscopy was first theoretically developed by Sheppard in 1980s. AiryScan microscopy from Zeiss efficiently implements ISM by collecting the emission spot with a GaAsP detector followed by post processing based on Sheppard summing. The GaAsP has 32 detectors arranged in a hexagonal arrangement as shown in **figure a**. Diameter

of the solid circle is 1.25 AU and diameter of the smaller circle is 0.2 AU. Airy Unit (AU) is the diffraction spread of a point emitter defined by,

$$AU = \frac{1.22 \times \lambda}{2 \times N.A} \quad (7.1)$$

where  $\lambda$  is the wavelength of emission light in nanometers and N.A is the numerical aperture of the objective. The ISM implemented in the AiryScan is based on considering each small detector in a GaAsP detector acting as a displaced pinhole of a confocal microscope. There are four rings in the GaAsP detector structure, with the first detector/first ring in the centre or along the optical axis. Intensities collected in the other detectors located in 2<sup>nd</sup>, 3<sup>rd</sup> and 4<sup>th</sup> rings are equivalent to the intensity collected with a displaced pinhole, displaced from the optical axis. When the Airy disk of the emission PSF hits the detector, 32 images are generated with each image corresponding to the intensity detected by each small detector. Each of the 32 images is deconvoluted separately using Wiener deconvolution and then weighed summing of these 32 images results in an AiryScan image.

AiryScan equivalent image using any camera based confocal set up is generated by considering each pixel in the camera as an analog of the small detectors in a GaAsP detector. Data can be collected using any multifocal confocal setup using a DMD or spinning disk or any single spot confocal set up using laser scanning can be used. We divide the rectangular camera detector arrangement into four rectangles (equivalent to the four rings in a GaAsP detector).



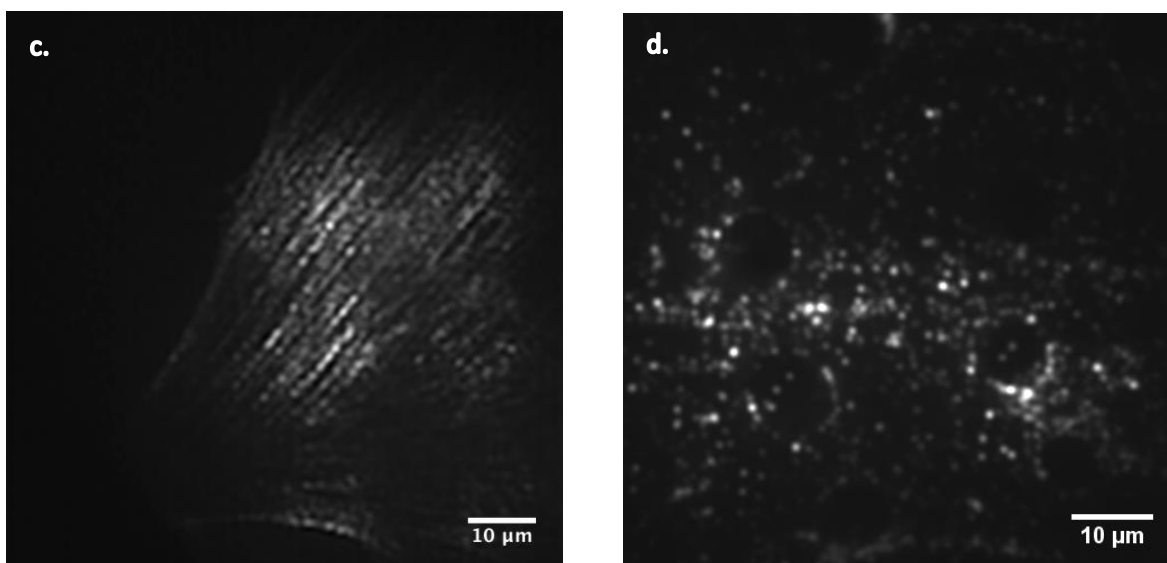
Due to the hexagonal arrangement of the GaAsP detector all the detectors in one ring are equidistant from the centre detector or optical axis while all the pixels in one rectangle are not equidistant from the centre or the optical axis. This is compensated with different weights for pixels depending on their location in the camera with respect to the optical axis. There are 49 displaced pinholes divided into 10 different weights (figure b). All the pixels which are numbered with the same number are displaced at same distance from the centre. Depending on the location of the pixels or displaced pinholes, we calculate its contribution to the final image.

The emission wavelength is 505 nm with 100x magnification, 1.49 N.A oil objective for the data acquired to reconstruct the image in **supplementary note 7 figure (c) and (d)**. With this setting,



one AU is 212.44 nm. Andor sCMOS Zyla 4.42 camera is used in this optical setup which has a pixel size of 65 nm. Detector area in this camera based Airy imaging is 7x7 pixels which is 455 nm and covers the full Airy disk of the emission PSF of a point emitter.

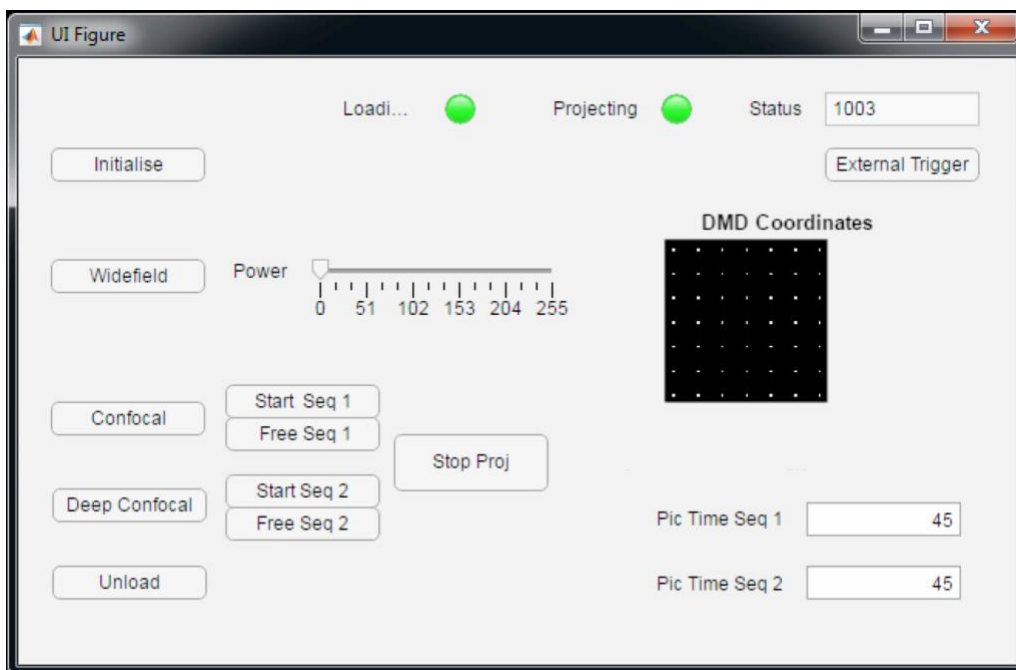
Here, it is worth recalling that SR-PAM optical set up collects both in-focus and out-of-focus emission spots in two separate cameras. In AiryScan, since there is no physical pinhole to reject the out-of-focus light in the emission pathway, we add the in-focus and out-of-focus emission spots to restore the complete emission spot and then run the data through our algorithm for camera AiryScan to obtain the AiryImage. **Supplementary note 7 figure (c) and (d)** are AiryImages obtained using this technique. This algorithm uses the DMD-camera calibration method detailed in **supplementary note 4** to find the coordinates of each emission spot. For setups which are not based on DMD illumination, such as a spinning disk or laser point scanning setups can use algorithms such as ThunderSTORM [4], rapidSTORM [5] to find the emission spot coordinates in the camera. Codes for obtaining AiryImages with any confocal optical set up is open access with paper and is given supplementary code. Equivalently, an MSIM image can be easily obtained with the SR-PAM set up and algorithm by summing the in-focus and out-of-focus emission spot and performing ISM followed by deconvolution.



## Supplementary Note 8. DMD Projection Control Software

GUI of the DMD pattern projection software open source with this paper is given in the **supplementary note 8 figure**. It has three patterns loaded. This can be extended to any number of patterns with different pinhole sizes and inter pinhole distances. First pattern is widefield illumination with all DMD pixels ON. The power of illumination can be controlled by the power slider. Second pattern is a 3x3 DMD pixels pinhole size with inter pinhole distance 3x5 DMD pixels. This pattern is loaded in binary format. This can be used to run the DMD at the fastest

frame rate which is 44  $\mu$ sec per frame for rapid confocal scanning. Third pattern is the deep confocal with 3x3 DMD pixels pinhole size with inter pinhole distance 3x10 DMD pixels to image deep areas of thick samples.

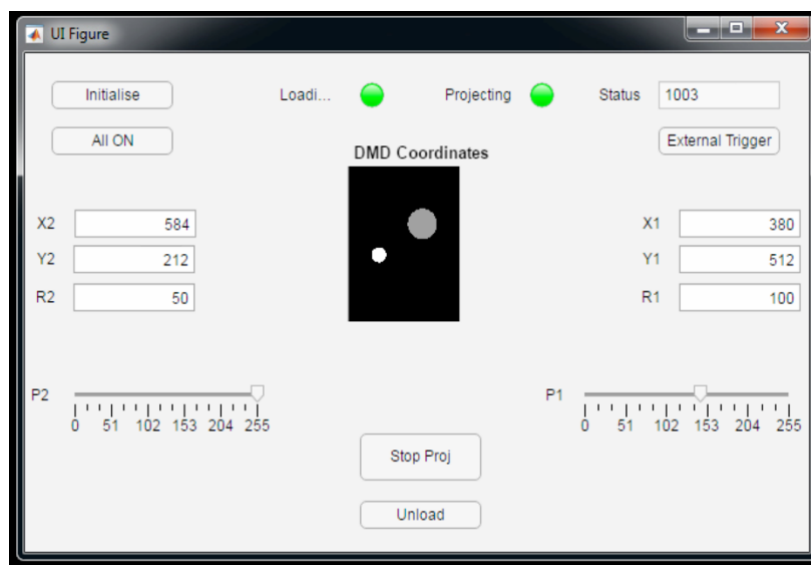


## Supplementary Note 9. Targeted Illumination Software

Targeted illumination has been used in optical microscopy to manipulate and explore various cellular dynamics and structures. There are many techniques which exploit targeted illumination including optogenetics, Florescence Recovery After Photobleaching (FRAP), photoactivation, ablation, photo-conversion, uncaging etc. Development of targeted illumination software and its implementation into the optical set up described in this section is a tool which can be easily implemented and widely adapted to these applications.

This section outlines the development of the software written in MATLAB programming language for targeted illumination system using DLP technology. To test the performance and to establish the application of the system, the technique is applied for the selection of a single channel in a mother machine system and to selectively illuminate specific bacteria of interest. The mother machine is a microfluidic system to study generations of bacteria in balanced growth conditions for long term imaging. E.coli cells expressing GFP are imaged to demonstrate the capabilities of the system. Software for targeted illumination presented in this section can be widely adopted with any DMD based set up without the need for the SR-PAM optical set up. Power and pattern of light illumination is precisely controlled using the software.

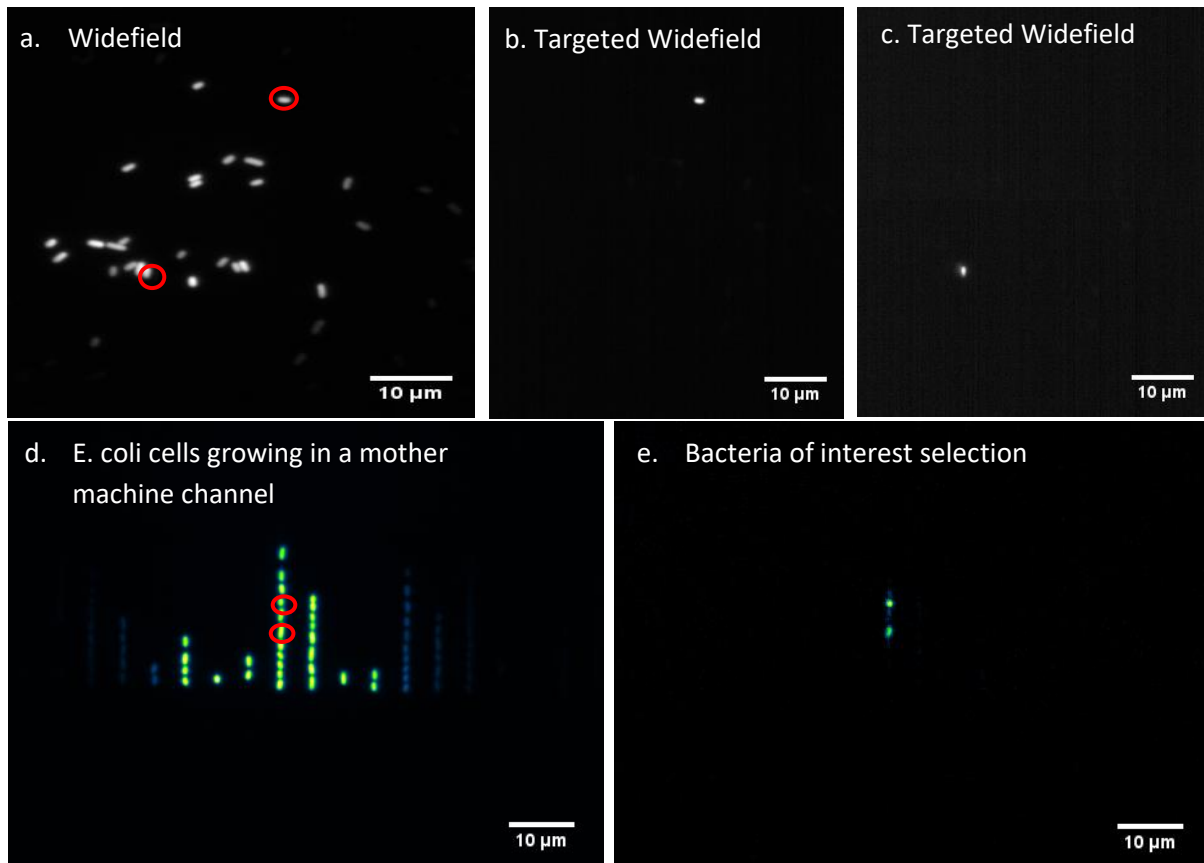
Custom made GUI made for illuminating only a selected number of bacteria. GUI in **supplementary note 9 figure** below allows the user to illuminate only a selected area of interest in the sample. Circular shape is chosen considering the shape of the bacteria for investigation. The user can move the centre and radius of the circle to move the area of illumination along the field of view of the sample so that only the bacteria of interest are illuminated. Since the image loaded on to the memory of DMD is in MSB format, grey scale level of circles can be conveniently changed. User can also define the power with which the area is illuminated by changing the power slider from 0 to 255.



In this example, bacteria of interest were selectively illumination using the GUI. GUI used for this experiment is based on projecting two circles with the centre position and radius defined by the user. After taking the widefield image, DMD coordinates for the centre of the circles and the desired radius of the circles to be projected can be given as an input in the GUI. The circles can be loaded on to the onboard memory and projection can be started by pressing 'Enter' in the keyboard. Power of illumination intensity can be controlled by a sliding button. Power slider number 0 corresponds to the DMD in 'OFF' state or the micromirror turned to the pathway opposite to illumination, and 255 corresponds to the DMD in 'ON state or the micromirror turned towards the illumination pathway directing 100% of the illumination light towards the microscope. Number between 0 and 255, micromirrors flip between +12 and -12 to control the intensity of light illumination.

**Supplementary note 9 figure (a)** is a widefield image of E.coli expression GFP illuminated with 470 LED along one of the illumination pathways of the system. **Supplementary note 9 figures (b-c)** are targeted widefield images of the bacteria of interest. **Supplementary note 9 figure (c)** shows that adjacent E.coli cells can be selected and illuminated efficiently using the system. **Supplementary note 9 figure (d)** shows

a wide field image of bacteria lined up in various channels of mother machine and **Supplementary note 9 figure (e)** shows two E.coli cells in a channel are selected and illuminated.



**Supplementary note 9 fig. (a).** Wide field image of E.coli. **(b-c)** selectively illuminating bacteria of interest **(d)** Growing E.coli cells lined up in mother machine channels. **(e)** Two E.coli cells of interest are selectively illuminated.

GUI can be changed to project any pattern. A rectangular pattern determined by the position of the channel of interest in a mother machine is projected on the DMD. Channel position can be changed to illuminate any channel of interest in a mother machine. **Supplementary note 9 figure f** is E.coli cells growing in a mother machine channel and **Supplementary note 9 figure g** is the targeted illumination of a single channel.



**Supplementary note 9 fig.** (e) Wide field image of E. coli cells, (f) Single channel in mother machine selectively illuminated.

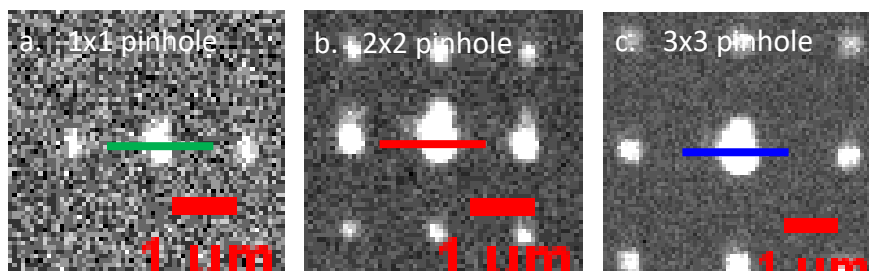
### **Supplementary Note 10. Pinhole size and intensity analysis**

The adaptive confocal implemented here can change between the pinhole size and inter pinhole distances conveniently by creating different patterns. Depending on the sample characteristics which determine the resolution required, speed of imaging and optical sectioning, various patterns

can be employed. For thick samples, larger inter pinhole distances can reduce the collection of scattered light from out-of-focus planes to pass through the pinholes. Large inter pinhole distance can also reduce the cross talk between the pinholes for thick samples. As the inter pinhole distance increases, optical sectioning ability of the microscope also increases. Smaller inter pinhole distance reduces the number of frames required for performing a complete scan. This increases the speed of imaging which may be more suitable for visualizing the dynamics in live cell imaging.

Another key factor considered here is the size of the pinhole. When the size of the pinhole is small, for example, when 1x1 DMD pixel is used as one pinhole, the intensity of light projected, and the intensity of light collected through the pinhole are less. This is shown as the green curve in **supplementary note 10 figure (d)**. With a medium sized pinhole, for example, when 2x2 DMD pixels are used as one pinhole, the intensity of light projected, and the intensity of light collected through the pinhole are higher than 1x1 DMD pixel pinholes as shown as the red curve in **supplementary note 10 figure (d)**. 3x3 DMD pixels when used as a pinhole project higher excitation intensity on to the sample and collect higher emission intensity from the sample. Emission intensity of 3x3 DMD pixels pinhole is shown as blue curve in **supplementary note 10 figure (d)**. This is ideal to samples with low fluorescence emission intensity. When using a 100x objective, 1x1 projects 136 nm size spot, 2x2 projects 272 nm size spot and 3x3 projects 408 nm spot in the sample plane ignoring the diffraction limit. Due to the diffraction limited system, a point emitter will have ( $\frac{\lambda}{2*NA} = 168 \text{ nm}$ ) diffraction spread with widefield illumination.

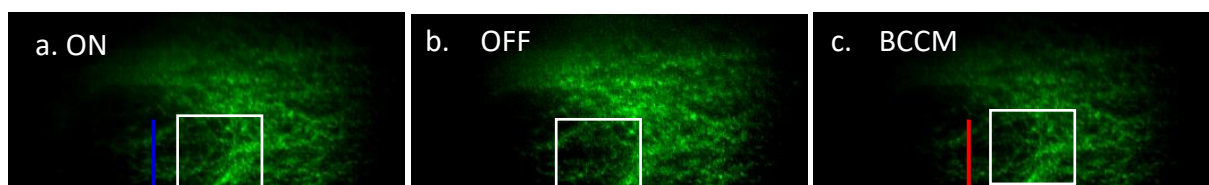
**Supplementary note 10 figure** is a comparison of different confocal projection patterns employed in this work. Three different multifocal illumination patterns were projected on to a bead sample and the intensity collected for each pinhole was compared. **Supplementary note 10 figure (a)** is 1x1 DMD pixel with inter pinhole distance 1x10. **Supplementary note 10 figure (b)** is 2x2 DMD pixels with inter pinhole distance 2x5. **Supplementary note 10 figure (c)** is 3x3 DMD pixels with inter pinhole distance 3x5. **Supplementary note 10 figure (d)** is the intensity profile of line through the data collected with the three different patterns. Intensity of emission light collected increases as the pinhole size increases. FWHM of 1x1 emission pinhole is 160 nm, 2x2 is 250 nm and 3x3 is 370 nm.



**(Supplementary note 10 fig. Comparison of emission intensity with different confocal projection patterns. (a) 1x1 pinhole with inter pinhole distance 1x10. (b) 2x2 pinhole with inter pinhole distance 2x5. (c) 3x3 pinhole with inter pinhole distance 3x5. (d) Intensity profile of line through 1x1, 2x2 and 3x3 pinholes)**

## **Supplementary Note 11. Background Corrected Confocal Microscope**

To demonstrate the background subtraction in the system without post processing of SR-PAM, microtubules were imaged. Background Subtracted Confocal Microscope is the SR-PAM data reconstructed without resolution doubling. Multifocal pattern with 3x3 pinhole size and 3x5 inter pinhole distance was projected onto the sample to collect in-focus and out-of-focus data in two separate cameras as described in the previous sections.



**(Supplementary note 11 fig. Background Corrected Confocal Microscopy imaging on microtubules. (a)** Sum of all the frames collected in ON image. **(b)** Sum of all the frames collected in OFF image. **(c)** Image reconstructed with BCCM algorithm. **(d)** Line profile through ON image. **(e)** Line profile through BCCM image. **(f), (g), (h)** Zoomed in areas of figure **(a), (b), (c)**. **(i)** Normalized intensity profile of lines through one microtubule in ON, OFF and BCCM.)

**Supplementary note 11 figure (a), (f)** are the sum of all the frames collected in ON camera and **supplementary note 11 figure (b), (g)** are the sum of all the frames collected in OFF camera.

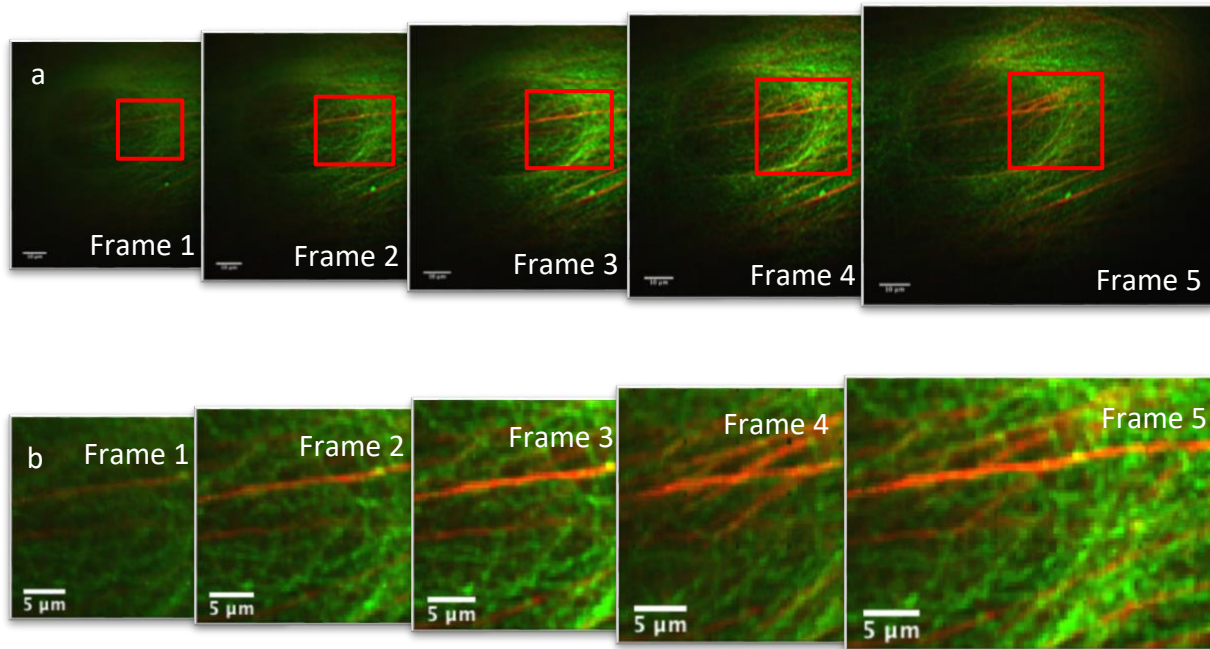


**Supplementary note 11 figure (c), (h)** are the BCCM image. It can be seen in the BCCM image that, it shows higher background subtraction with microtubule structures more prominent. Figures d and e are intensity profiles through ON and OFF images as shown by blue and red lines in figure a and b respectively. Black arrows indicate the places where there is a higher signal-to-noise ratio or higher distinction of adjacent structures. **Supplementary note 11 figure (f), (g), (h)** are the zoomed in images of areas in **Supplementary note 11 figures (a), (b), (c)** marked as shown by white squares. Line profile through one microtubule structure in ON, OFF and BCCM image was taken as shown in **Supplementary note 11 figure (i)**. FWHM of microtubule width obtained in ON image is 460 nm, OFF image is 610 nm and BCCM image is 430 nm.

## **Supplementary Note 12. Dual colour in BCCM mode**

To explore the potential of BCCM for dual color imaging with Z stack, microfilaments of bovine pulmonary artery endothelial (BPAEC) cells were imaged. Samples were labelled with Texas Red-X phalloidin for F-actin and anti—bovine  $\alpha$ -tubulin mouse monoclonal 236-10501 in conjunction with BODIPY FL goat anti—mouse IgG antibody was labelled microtubules. Prepared slide was purchased from Thermofishers (product number-F14781). This is the same sample used for the images in **supplementary note 11**.

Multifocal patterns with pinhole size 3x3 DMD pixels and inter pinhole distance 3x5 DMD pixels were employed. ON and OFF data were collected for 5 slices. Sample stage is moved axially to change the z position of the sample by controlling the stage using piezo z-stage controller with LabView as detailed in **supplementary figure 4**. Each slice was taken by moving the stage by 500 nm. Reconstruction was done with each colour separately and combined. **Supplementary note 12 figure (a)** is the dual colour microtubules and actin reconstructed with BCCM. **Supplementary note 12 figure (b)** is the red square zoomed in.



**Supplementary note 12 fig. Dual colour microtubules and actin z-stack.** (a), Frame 1 to 5. (b), Frames 1 to 5 red square zoomed in.

## Supplementary Codes

1. DMD projection code with patterns used in the paper
2. Targeted illumination software
3. Codes to build patterns
4. DMD camera calibration
5. Background Correction Confocal Microscope reconstruction
6. SR-PAM reconstruction code
7. AiryImaging codes

## Reference

1. Huygens deconvolution, SVI, <https://svi.nl/HuygensDeconvolution>.
2. Culley, S. et al. Quantitative mapping and minimization of super- resolution optical imaging artifacts. *Nat. Methods* **15**, 263-+ (2018).
3. Gustafsson, N. et al. Fast live-cell conventional fluorophore nanoscopy with ImageJ through super-resolution radial fluctuations. *Nature communications*. **7**, 12471 (2016).
4. Ovesný, M., Křížek, P., Borkovec, J., Švindrych, Z. & Hagen, G.M. ThunderSTORM: a comprehensive ImageJ plug-in for PALM and STORM data analysis and super-resolution imaging. *Bioinformatics* **30**, 2389-2390 (2014).
5. Steve, W. et al. rapidSTORM: accurate, fast open- source software for localization microscopy. *Nature Methods* **9**, 1040 (2012).